Journal of Geophysical Research: Oceans

RESEARCH ARTICLE
10.1029/2018JC014265

Surface Salinity Balance in the Tropical Pacific Off Mexico

Esther Portela[1,2], Emilio Beier[3], Eric D. Barton[4], and Laura Sánchez-Velasco[5]

[1]Centro de Investigación Científica y Educación Superior de Ensenada, Ensenada, Mexico, [2]Now at Laboratoire de Physique des Océans, Ifremer, Plouzané, France, [3]Centro de Investigación Científica y Educación Superior de Ensenada, Unidad La Paz, La Paz, Mexico, [4]Instituto de Investigaciones Marinas, Consejo Superior de Investigaciones Científicas, Vigo, Spain, [5]Departamento de Plancton y Ecología Marina, CICIMAR, Instituto Politécnico Nacional, La Paz, Mexico

Key Points:
- Salinity balance and its related processes are explained with a simple two-dimensional model
- The area's salinity decreases between June and October as a result of net precipitation and poleward advection of fresh tropical waters
- Mexican Coastal Current is the principal agent for salt advection between Tehuantepec and Cabo Corrientes

Supporting Information:
- Supporting Information S1

Correspondence to:
E. Portela,
estherinhabajoelmar@gmail.com

Citation:
Portela, E., Beier, E., Barton, E. D., & Sánchez-Velasco, L. (2018). Surface salinity balance in the tropical Pacific off Mexico. *Journal of Geophysical Research: Oceans*, *123*, 5763–5776. https://doi.org/10.1029/2018JC014265

Received 12 JUN 2018
Accepted 16 JUL 2018
Accepted article online 27 JUL 2018
Published online 18 AUG 2018

Abstract A simplified analytical model was used to solve the salinity balance equation and study the relative contributions of freshwater flux and salt advection to the salinity tendency between the Gulf of Tehuantepec and Cabo Corrientes (14–22°N). The model used climatological mixed-layer salinity, satellite-derived geostrophic velocity and evaporation minus precipitation data in a four-domain scheme. The mean circulation derived from the model largely coincides with previous reports and suggests that, in the steady state, the Mexican Coastal Current is decoupled from the Tehuantepec region. The analysis of the time-dependent variability showed that the salt advection can be largely explained by the annual variations of the alongshore velocity (corresponding with the Mexican Coastal Current) and an average salinity. At the seasonal scale, the salt advection and the freshwater flux have similar contributions to the resulting salinity tendency. Near Tehuantepec, due to a local salinity regime, the analytical model does not represent well the observations, while in Manzanillo and Zihuatanejo the agreement between the model and the observations is good in both amplitude and phase. The accuracy of the model in representing the observations is improved in the first third of the year by inclusion of the semiannual scale and the nonlinear processes in the equation of salt advection.

1. Introduction

The tropical Pacific off Mexico (TPOM) is located approximately between 14–22°N and 95–110°W. As the large zonal currents traveling across the Pacific Ocean (like the north equatorial countercurrent and NE subsurface countercurrent) reach the west coast of America, they redistribute producing three-dimensional structure product of the wind forcing and the shape of the American continent (Kessler, 2006; Wyrtki, 1965). Concretely, the TPOM is a particular region with complicated dynamics due to the confluence of different circulation regimes. The tropical branch of the California Current (Godínez et al., 2010) reaches the TPOM from the northwest carrying fresh and relatively cold water. From the southeast, the alongshore Mexican Coastal Current (MCC) brings fresh and warm water during summer and fall (Portela et al., 2016), and the seasonally variable, southeastward flow associated with the northern edge of the Tehuantepec Bowl borders the TPOM on the west (Godínez et al., 2010; Kessler, 2006; Lavín et al., 2006). The TPOM is significantly influenced by these different advective processes, but it is dominated by the alongshore circulation of the MCC that exhibits a strong seasonal behavior (Godínez et al., 2010). The different currents that converge in there, carrying water with very distinctive thermohaline properties, imprint their signature in the water masses of this region that are also modulated by the heterogeneity of the atmospheric conditions at the northern and southern edges of the TPOM. Its northern part lies in a tropical-subtropical transition zone where the evaporation exceeds the freshwater input (precipitation + runoff) throughout the year except in summer (Portela et al., 2016). The southern TPOM is strongly influenced by the seasonal winds blowing intermittently through the mountain gaps at the Tehuantepec isthmus (Amador et al., 2006; Romero-Centeno et al., 2003). In this southern region there is net freshwater input into the ocean between May and October while, due to the strength of the winds, net evaporation occurs between November and April (Fiedler & Talley, 2006; Portela et al., 2016).

The seasonality of the currents that converge in the TPOM largely determines the distribution of the regional water masses. However, little is known about the role that the freshwater flux plays in the modulation of the contrasting salinity features in this region.

Salinity's contribution to the stratification of the water column has an important influence on the oceanic circulation and on the tropical climate (Da-Allada et al., 2013; Foltz & McPhaden, 2008). Departures from a mean $T - S$ relation can have significant effects on dynamic height variations and therefore on the geostrophic

velocity and the heat transport (Johnson et al., 2002). Salinity has an important effect in a multidisciplinary sense: it affects the solubility of the CO_2 in the seawater and therefore its spatial distribution and related biological properties as the distribution primary producers (Franco et al., 2014).

The salinity balance has been studied with different approaches, including numerical models (Da-Allada et al., 2013; Z. Yu et al., 2008), observational in situ data (Beron-Vera et al., 2008; Cronin & McPhaden, 1998; Delcroix et al., 1996; Dessier & Donguy, 1994; Johnson et al., 2002; Montes et al., 2015; Ren & Riser, 2009), and satellite data in combination with the above (Dong et al., 2009; Foltz & McPhaden, 2008; Yu, 2011).

It is known that freshwater flux and oceanic dynamical processes are the main factors driving the variability of salinity throughout the world oceans (Johnson et al., 2002; Yu, 2011), but their relative importance is variable both in time (Da-Allada et al., 2013) and space. In regions of heavy rainfall or high evaporation the freshwater flux governs the mixed-layer salinity budget while the dynamical processes are dominant mainly outside the tropics (Yu, 2011). In the eastern tropical Pacific (ETP), Delcroix et al. (1996) found a large and negative correlation between the sea surface salinity and precipitation, while they were uncorrelated in the western equatorial Pacific.

In the open ocean, the magnitude and spatial patterns of salt advection at climatological time scales should largely match those of the mean freshwater flux to achieve a salinity balance (Dessier & Donguy, 1994). While it is true for several regions of the global oceans (Johnson et al., 2002; Yu, 2011), in others, it is not. Throughout most of the tropical North Atlantic, the sum of salt advection and freshwater flux underestimates the mixed-layer salinity tendency during fall and winter (Foltz & McPhaden, 2008). These authors suggested that regional processes as the entrainment could account for this imbalance. In this, and other studies (Dong et al., 2009; Johnson et al., 2002; Ren & Riser, 2009), the errors in the calculations of salinity advection have been related to the lack of high-resolution salinity data.

The above studies were carried out over long, even basin-wide, spatial scales on grids too coarse to resolve the processes at the coastal margins. The global scarcity of salinity data of adequate spatial resolution has limited the number of studies in coastal regions other than coastal lagoons (Kjerfve et al., 1996). Within the ETP there are only two such studies (Beron-Vera & Ripa, 2002; Montes et al., 2015) of this characteristics carried out in the Gulf of California, a semi-enclosed, very well sampled sea that borders the TPOM on the north.

Thanks to the effort made in gathering new, high-resolution, salinity data, this study contributes to the knowledge of the ETP by providing new information on the salinity balance in the TPOM. The results presented here on the relative importance of the freshwater fluxes and the main surface dynamical processes at climatological time scales in the region are important for future multidisciplinary studies involving physical and geochemical properties and plankton distribution.

2. Methods

2.1. Data

The hydrographic database is composed of profiles from CTDs, bottles, and profiling floats obtained from the World Ocean Database 2013 (https://www.nodc.noaa.gov/OC5/WOD13/data13geo.html) that span between 1939 and 2015, plus CTD data from 30 cruises of different sources carried out between 1992 and 2015. In addition, surface temperature and salinity data collected with a thermosalinograph (Philbrick et al., 2001) were provided by National Oceanic and Atmospheric Administration (NOAA) Fisheries, Southwest Fisheries Science Center (see data distribution and timeline in Portela et al., 2016).

The atmospheric data of evaporation minus precipitation ($E - P$) were provided by the National Centers for Environmental Prediction Climate Forecast System Reanalysis (CFSR), Research Data Archive at the National Center for Atmospheric Research (NCAR), Computational and Information Systems Laboratory. These are 6-hourly gridded products of data reanalysis from 1979 onward with a spatial resolution of 0.5° × 0.5° of latitude and longitude. The CFSR product is the one with better spatial and temporal resolution among other 10 reanalyses analyzed by Yu et al. (2017). This is the only product that features a weakly coupled atmosphere-ocean-land reanalysis, while the others are only atmospheric. This feature has a potential for better depiction of the overall atmosphere-ocean feedback processes than the uncoupled data assimilations (Wen et al., 2012). In addition, CFSR implemented corrections in the precipitation model using observational data that distinguish it from other reanalysis products (L. Yu et al., 2017).

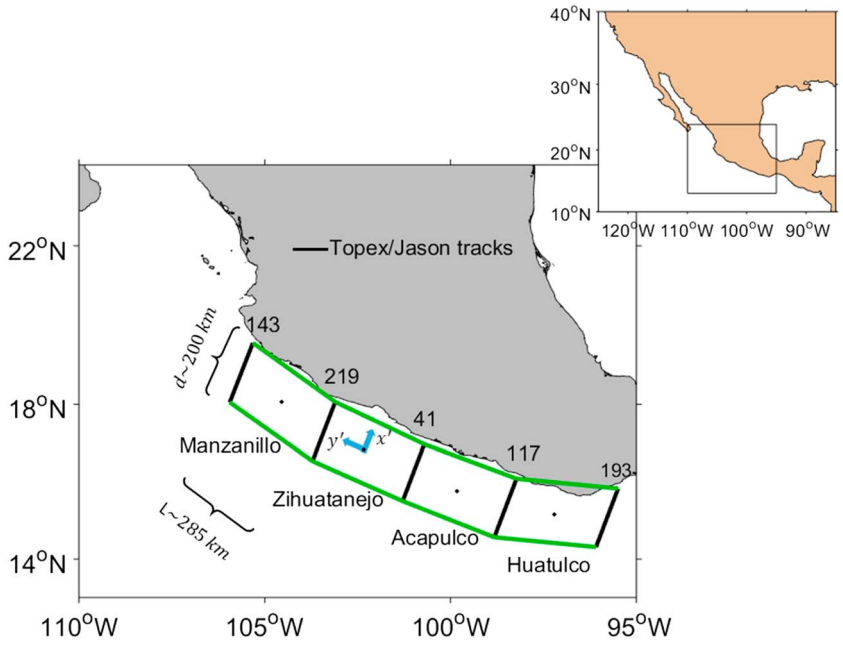

Figure 1. Schematic representation of the study area (inset) and the model domains (main figure). The black lines are the satellite tracks that are labeled with their original numbers. The green lines represent the limits of the domains.

The monthly climatological discharge of the 21 most important Mexican rivers discharging into the Pacific Ocean was obtained from the Global Runoff Database, provided by the Global Runoff Data Centre of the Federal Institute of Hydrology (BfG). We found that in our study area, from the northwestern side of the Gulf of Tehuantepec (GoT) to the south of Cabo Corrientes, the river discharge contribution was lower than 6% of the total freshwater input (not shown). For this reason, the runoff was excluded from the calculations of the freshwater balance.

Absolute dynamic topography was obtained from five ascending-pass tracks of the Topex/Jason satellite. These data are developed, validated, and distributed by the Center for Topographic studies of the Ocean and Hydrosphere (CTOH)/Laboratoire d'Etudes en Géophysique et Océanographie Spatiales (LEGOS), France. The complete time series lasts from 1993 to 2016. Although typically, the satellite altimetry products have uncertainties near the coast (Saraceno et al., 2008), these data are processed with specific corrections that improve the data quality in coastal areas. Among other advantages, the width of the coastal band of non-valid data is narrower than in the normal along-track altimetry product. This processing includes improved tide, wind, and pressure corrections.

2.2. Data Analysis

Potential temperature and practical salinity were converted into conservative temperature (Θ) and absolute salinity (S_A) following the Thermodynamic Equation of Seawater 2010 (TEOS-10). According to McDougall and Barker (2011), S_A and Θ must be used in scientific publications since the S_A takes into account the spatially varying composition of seawater and Θ represents more accurately its heat content per unit mass. These improvements account for 10 times the precision of the former equation of state for seawater-80, and they were recommended by Intergovernmental Oceanographic Commission in 2010.

The mean mixed-layer depth (MLD) in each season and in four spatial domains along the coast (Figure 1) was calculated following the method of Kara et al. (2000). The S_A and MLD data were gridded to obtain monthly climatology maps with a resolution of 0.25° × 0.25°. The mixed-layer salinity was obtained by averaging all the available measurements within a constant MLD in each cast. Then salinity, MLD, and the $E - P$ fields were interpolated onto the satellite track locations.

The annual and seasonal (annual + semiannual) signals of every variable were estimated by fitting their corresponding harmonics following the mean square fit method as indicated in equation (1).

$$H_a(\vec{X},t) = A_a(\vec{X})\cos\left(\omega t - \varphi_a(\vec{X})\right) \quad (1)$$

$$H_s(\vec{X},t) = A_s(\vec{X})\cos\left(2\omega t - \varphi_s(\vec{X})\right) \quad (2)$$

where $\vec{X} = X(x,y)$, H refers to the harmonic of a particular variable that is either annual (a) or semiannual (s), A is the amplitude, φ is the phase, ω is the radian frequency $2\pi/12$ months, and t is the time referred to the beginning of the year.

3. Analytical Model

In order to study the salinity balance and describe the relative contribution of each term to the salinity change rate (hereinafter salinity tendency), we used an inhomogeneous, salt advection model adapted from the works of Dong et al. (2009), Da-Allada et al. (2013), and Yu (2011). We considered that the salinity tendency (left-hand side of the equation (3)) responds to a balance between freshwater flux and oceanic dynamical processes composed of salt advection, entrainment, and mixing (the four terms of the right-hand side of equation (3), respectively).

$$\frac{\partial S}{\partial t} = \frac{S_o}{H_o}(\mathrm{E}-\mathrm{P}) - (\mathrm{U}\cdot\nabla_h S) - \frac{S-S_h}{H_0}H(w_e) + \kappa\nabla^2 S \quad (3)$$

H_0 is the reference MLD and S_0 is the reference salinity, both were obtained as the spatial and temporal mean of MLD and S_A, respectively. U and S are the mixed-layer horizontal velocity and salinity and S_h is the salinity just below the MLD. κ is the diffusion coefficient, set to 500 m s^{-2} following Yu (2011). $H(w_e)$ is the Heaviside function that equals the entrainment velocity: $H(w_e) = w_e$ only when there is an increase of the MLD, otherwise $H(w_e) = 0$. The entrainment velocity is defined as the mixed-layer deepening rate plus the vertical velocity.

Each term in equation (3) was decomposed into the mean and the time-dependent variability. Although perturbations to the steady state occur on many time scales, the focus here is on the annual and seasonal signals of the climatology since these time scales explain the greater part of the nearshore variability in the study area (Godínez et al., 2010).

The model was applied to a four-domain scheme delimited by five Topex/Jason tracks (Figure 1). The satellite tracks represent the border between each domain as well as the southeast and northwest limits of the whole area. The coordinate system was defined to have a component parallel (x') and other perpendicular (y') to the satellite tracks that are positive coastward and northwestward, respectively (Figure 1). The velocity components associated to the x' and y'axes approximate to the flow perpendicular and parallel to the coast, respectively.

Each domain is approximately 200 km wide and 285 km long. Although the differences in the orientations of the five tracks imply that the definition of the axis directions vary from one domain to another and the dimensions of the domains are not exactly equal, these differences do not have any significant effect on our results. The resulting values of each term of equation (3) are located at the center of the boxes, as indicated by the black dots in Figure 1.

The first aim of this work is to understand the main mechanisms driving the salinity changes and, concretely, the salt advection. To this end, the first approximation was a simple balance between the freshwater flux and the salt advection as proposed by (Delcroix et al., 1996; Johnson et al., 2002) to analyze the steady state and the annual salinity tendency. Entrainment and mixing will be neglected at first instance and added to the equations when addressing the seasonal salinity balance in order to identify some of the sources of the residual imbalances.

Preliminary results showed that the salt advection in the direction perpendicular to the coast is around 2 orders of magnitude lower than along the coast ($v'\frac{\partial \overline{S}}{\partial y} \sim 10^{-7}$ (g kg^{-1} s^{-1}) while $u'\frac{\partial \overline{S}}{\partial x} \sim 10^{-9}$ (g kg^{-1} s^{-1})).

Given the low contribution of this across-shore term, salt advection will be approximated by its alongshore component only (by the MCC) and the velocity component perpendicular to the coast, u, will be set to zero. This approximation will be taken in account as part of the imbalance of the model. To isolate the effect of the

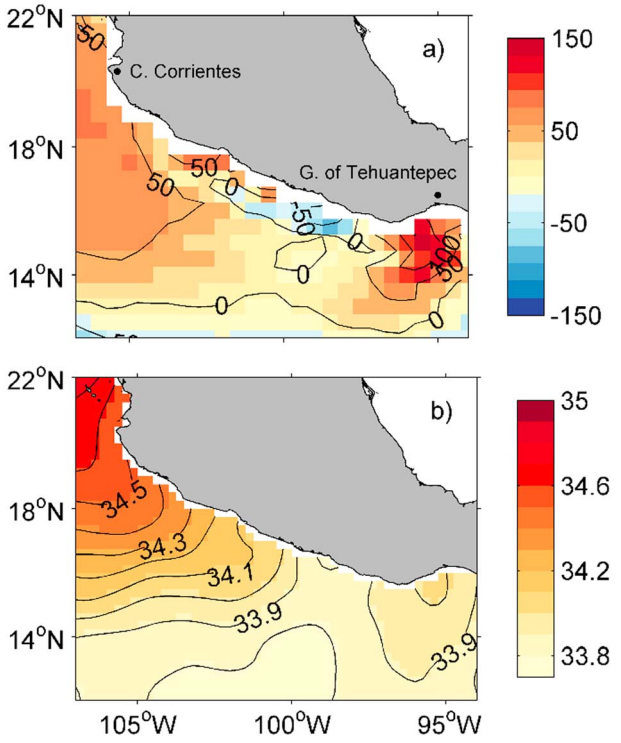

Figure 2. Mean values of the (a) $E - P$ (cm year^{-1}) and (b) salinity (g kg^{-1}) in the study area.

MCC, the study area extends 200 km from the coast. This is wide enough to include both the observed (Lavín et al., 2006) and modeled (Pantoja et al., 2012) width of the MCC.

In the steady state, the mean $E - P$ and salinity were obtained directly from observations, but the mean velocity was derived indirectly from the satellite altimetry. The absolute dynamic topography is obtained as the sum of mean dynamic topography (MDT) and sea level anomaly. While the sea level anomaly is measured by the satellite, the MDT is an estimated quantity subject to continuous improvement. It is well defined at large spatial scales, but its reliability at regional scale depends on the quality and availability of the in situ data and it has not been generally validated. Our study area is a coastal, poorly sampled region, and so the MDT and the geostrophic velocity derived from it are locally unreliable. A better alternative is to estimate the mean, modeled, alongshore component of the velocity ($\overline{v}_m$) from the model assuming that $\overline{U} = (\tilde{}0, \overline{v})$:

$$0 = \frac{S_o}{H_o}\left(\overline{E-P}\right) - \overline{v}_m \frac{\partial \overline{S}}{\partial y} \tag{4}$$

$$\overline{v}_m = \frac{\frac{S_0}{H_0}\left(\overline{E-P}\right)}{\frac{\partial \overline{S}}{\partial y}} \tag{5}$$

3.1. Analysis of the Advection

While obtaining the anomalies of the freshwater flux is straightforward, the nonlinearity of the advective term needs to be analyzed thoroughly. We first split the salt advection into its four components obtained by separating the mean state from the time-dependent variability or perturbations. These perturbations will be then analyzed as the annual and seasonal scales separately:

$$v\cdot\nabla_h S = \left(\overline{v} + v'\right)\cdot\nabla_h\left(\overline{S} + S'\right) \tag{6}$$

$$v\cdot\nabla_h S = \underbrace{\overline{v}\cdot\nabla_h\overline{S}}_{\text{I}} + \underbrace{v'\cdot\nabla_h S'}_{\text{II}} + \underbrace{\overline{v}\cdot\nabla_h S'}_{\text{III}} + \underbrace{v'\cdot\nabla_h\overline{S}}_{\text{IV}} \tag{7}$$

The terms of the right-hand side in equation (7) hereinafter will be referred to as I, II, III, and IV in order from left to right.

Term I is the mean salt advection, term II is the advection of the mixed-layer salinity anomaly by the annual perturbation of the velocity, term III denotes the advection of the perturbed salinity by a mean velocity, and Term IV is the advection of the mean mixed-layer salinity by the perturbed velocity. The mean alongshore velocity, when it was implied in the calculations, was introduced as the $\overline{v}_m$ defined in equation (5).

The same criterion was applied to the entrainment term, in which case we neglected the products of anomalies for being more than one order or magnitude smaller than the other entrainment terms (not shown).

4. Results

4.1. General Overview

The mean climatology of $E - P$ shows that, in general terms, in the study area the evaporation exceeds precipitation (Figure 2). An exception is the small region of net precipitation located northwest of the GoT that coincides approximately with the domain of Acapulco.

Salinity decreases southeastward from its maximum (~34.8 g kg^{-1}) at the entrance of the Gulf of California, north of Cabo Corrientes, to minimum values of 33.8 g kg^{-1} at the northwestern edge of the GoT (Figure 2b). Slightly increased salinity is found again in the GoT coincident with the region of intense net evaporation in Figure 2a.

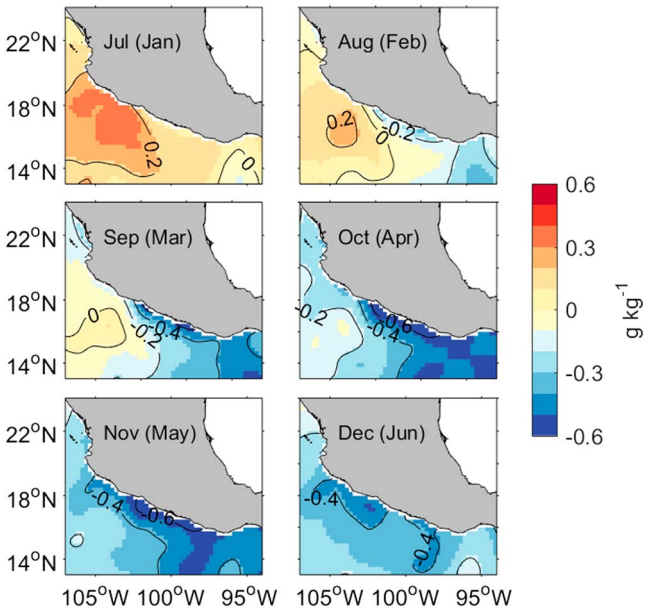

Figure 3. Annual surface salinity anomalies (g kg^{-1}) from July to December elaborated from the hydrographic database. The months with opposed phase in each panel are in parenthesis.

Figure 3 shows the annual salinity anomalies from July to December; because the annual cycle is symmetric, only half the year is shown in this figure and similar figures. Negative salinity anomalies in the coastal strip coincident with the model domains are observed between August and January. The minimum (maximum) salinity occurs northwest of the GoT between October and November (April and May), while near Cabo Corrientes it takes place between November and December (May and June). The lag between the occurrences of the peaks in both extremes of our domains is about 1 month.

The annual signal of the alongshore component of the velocity in the first 200 km offshore (Figure 4) shows a poleward flow from May to October, with maximum velocities between July and August (note that the reference arrow is not the same size in each subplot).

4.2. Mean Salinity Balance

From the steady state approximation of the salinity balance (Figure 5) we obtained the mean freshwater flux (Figure 5a), the alongshore salinity gradient (Figure 5b), and $\overline{v}_m$ (Figure 5c) within the four model domains. Net evaporation occurs in Manzanillo, Zihuatanejo, and Huatulco (Figure 5a), while Acapulco is situated on the small coastal region with local net precipitation observed in Figure 2a. The mean salinity increases poleward, from Acapulco to Manzanillo, and equatorward in Huatulco (Figure 5b).

The flow necessary for the alongshore salt advection to balance the freshwater flux, $\overline{v}_m$ (Figure 5c), is poleward in Zihuatanejo and Manzanillo, and equatorward in Huatulco, where the salinity changes in the opposite sense.

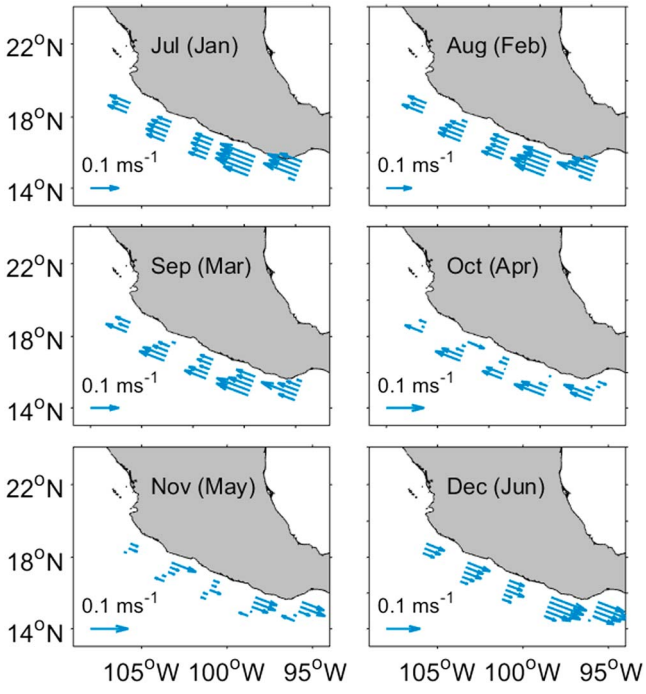

Figure 4. Annual signal of the alongshore component of the geostrophic velocity from July to December. The months with opposed phase in each panel are in parenthesis.

4.3. Temporal Variations

The climatology of $E - P$, salinity, and velocity shows strong annual cycles that represent between 59% and 84% of the total variance. The semiannual signal represents between 5% and 33% of the variance; it increases poleward and is the strongest in the case of the geostrophic velocity (Table 1).

While the annual signal provides the best way to identify the role of the main physical processes involved in the salinity balance, the seasonal signal accounts for the greater part of the time-dependent variability (between 88% and 97%) in our study area. The latter, therefore, is useful to examine how well the model represents the observations and to understand the contribution of the different factors to the observed tendency.

4.3.1. Annual Signal

The annual variability of the salt advection is given by terms III and IV of equation (7). In term II the product of two annual signals results mathematically in the sum of a mean value and a semiannual component. Since we are addressing in this section the perturbations of the mean state as the annual signal only, we excluded the latter term from our calculations. We will discuss this term II later, as part of the seasonal variations.

In Huatulco and Zihuatanejo term III (blue) is approximately half of the magnitude of term IV (green), while it is over an order of magnitude lower in Manzanillo and near zero in Acapulco (Figure 6).

In order to identify better the main dynamical processes involved in the salinity balance we will retain only the term IV of equation (7). This term

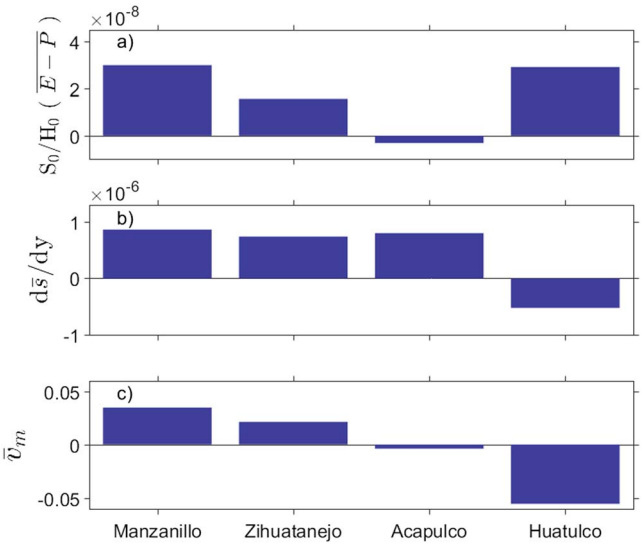

Figure 5. Mean value of the (a) freshwater flux term, (b) alongshore salinity gradient, and (c) mean, modeled alongshore component of the velocity ($\overline{v}_m$).

completely dominates the salt advection in Acapulco and Manzanillo while in Huatulco and Zihuatanejo it accounts for about 70% and 65% of the variance, respectively (Figure 7).

After the previously detailed approximations and subsequent linearization of the advective term, the annual cycle of the salinity balance can be expressed as follows:

$$\frac{\partial s'}{\partial t} = \frac{S_0}{H_0}(E-P)' - v'\frac{\partial \bar{s}}{\partial y} \tag{8}$$

where overbars denote the time mean and the primes denote the time-dependent variability.

The annual observed salinity tendency was calculated directly from the database and compared with the model result (Figure 8). The annual model approximates the amplitude (~70%) and phase (~90% and ~70%) of the salinity tendency in Manzanillo and Zihuatanejo. In contrast, in Acapulco, the model overestimates the observations by ~90% while the phase is around 20 days behind (Table 2). The maximum salinity gain is observed in mid-February in Manzanillo and the end of January in Zihuatanejo, while the maximum salinity lost takes place in mid-August and end of July, respectively. The salinity tendency in Huatulco is poorly described by the model that underestimates the amplitude and misses the phase in over a month.

Figure 9 shows the behavior of the freshwater flux and the salt advection terms, together with the resulting salinity tendency. Negative values represent excess of precipitation, poleward salt advection, and a decreasing salinity. Positive salt advection means that salinity is spatially increasing in the same direction as the flow, so that salinity at any point in this flow will decrease in time (that is revealed by the negative sign in front of the advection term in equation (3)).

The modeled salinity tendency shows a spatial continuity between Acapulco and Manzanillo, hereinafter the AM region. Poleward salt advection occurs between May and October with the maximum in August; net precipitation takes place between June and November, with the maximum between August and September. Resulting from the coincidence in phase of these two terms, the AM region loses salinity between June and October, while in May and November it remains practically constant.

In Huatulco, the freshwater flux is in phase with that of the AM region while the salt advection is in opposition (i.e., salinity increases poleward between May and October) and results in a smoother salinity tendency than in the observations (Figure 8).

4.3.2. Seasonal Signal

To identify possible causes of the disagreement between the model and the observations and improve the model accuracy, the semiannual harmonic was added to the annual one to obtain the seasonal salinity tendency in all four domains.

Since the approximations described for the annual scale are still applicable, the same criteria were used to obtain the linear seasonal model. In addition, the nonlinear term (term II), entrainment, and mixing were added in this analysis.

Table 1
Variance Explained (%) by the Annual (A), Semiannual (Sa), and Seasonal (S) Cycles of the Three Data Sets Implied in the Salinity Balance

	Manzanillo			Zihuatanejo			Acapulco			Huatulco		
	A	Sa	S	A	Sa	S	A	Sa	S	A	Sa	S
$E-P$	68	27	95	73	24	97	80	17	97	76	12	88
Salinity	77	15	92	81	11	92	83	8	91	84	5	89
Velocity	59	33	92	59	33	91	65	26	91	73	18	92

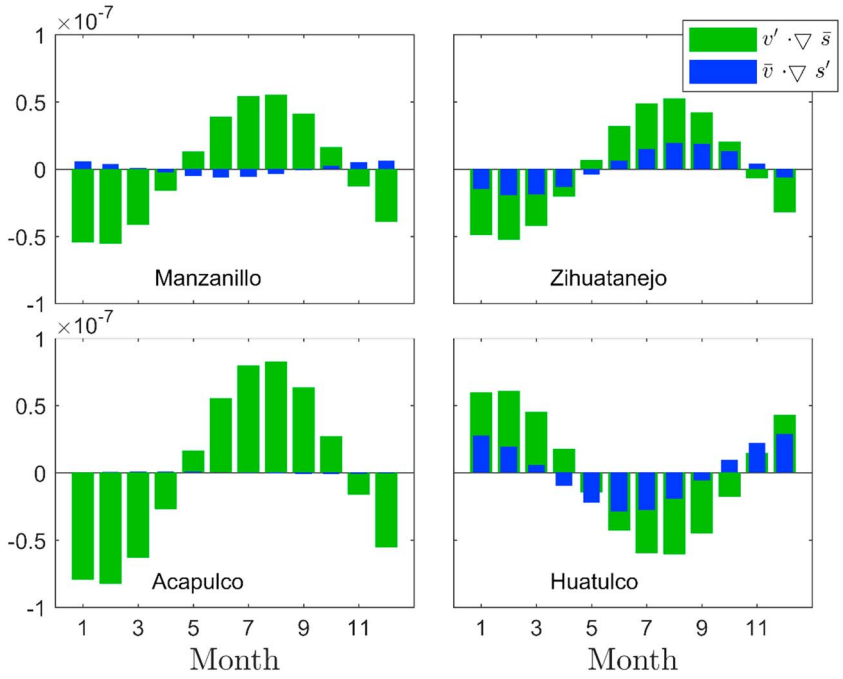

Figure 6. Comparison between the two terms of the advection that are responsible for its annual variations in each model domain. Term III ($\bar{v} \cdot \nabla_h S'$) in blue and term IV ($v' \cdot \nabla_h \bar{S}$) in green.

The relative importance of the salt advection, freshwater flux, and entrainment for the resulting salinity tendency was evaluated. The mixing term (~10^{-11}) was more than three orders of magnitude lower than the others (>10^{-8}), and therefore, it was not taken into account in future computations. In general, the contribution of the freshwater flux and salt advection to the salinity tendency is of the same order of magnitude (Table 3). However, while in the AM region they have similar values, in Zihuatanejo and especially in Huatulco, the freshwater flux predominates. The entrainment was much lower than the other two terms in all four domains, and it played a significant role only in Acapulco where it represented 13% of the total variance.

Comparing the observed and the modeled seasonal, salinity tendencies (Figure 10) indicates that in the AM region the linear seasonal model reproduces well the observations from May to January, while between February and April it overestimates the amplitude and misses the phase of the observations.

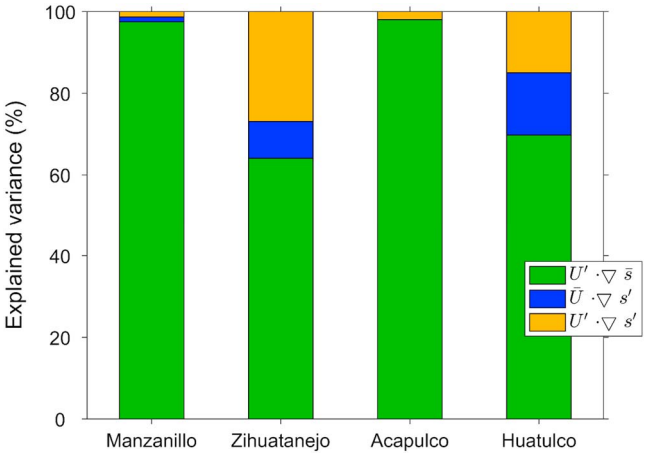

Figure 7. Variance explained by each of the three terms (term II in yellow, term III in blue, and term IV in green) of the salt advection in each domain of the annual model.

The linear model is especially accurate in Manzanillo and Zihuatanejo, Acapulco shows the greatest discrepancies, mainly in the amplitude, while in Huatulco the phase is poorly represented; the observed salinity tendency shows continuity with the AM region, but the model only approximates the observations between September and March.

The seasonal, nonlinear modeled salinity tendency (Figure 10, yellow line) resulting from the addition of the term (II) of equation (7) shows that, in general, the nonlinear advection occurs in the first third of the year, when it reduces the amplitude and therefore the differences between model and observations. The greatest importance of the nonlinear processes is evident in Huatulco where their addition changes the phase of the salinity tendency and improves the accuracy of the model between July and September and between January and March. As expected, the nonlinear term is unimportant in Manzanillo. In Acapulco, the seasonal model still overestimates the observations; however, the phase is accurate between May and January.

The addition of the entrainment only had a noticeable effect in Acapulco, during summer, when it smooths the salinity tendency and

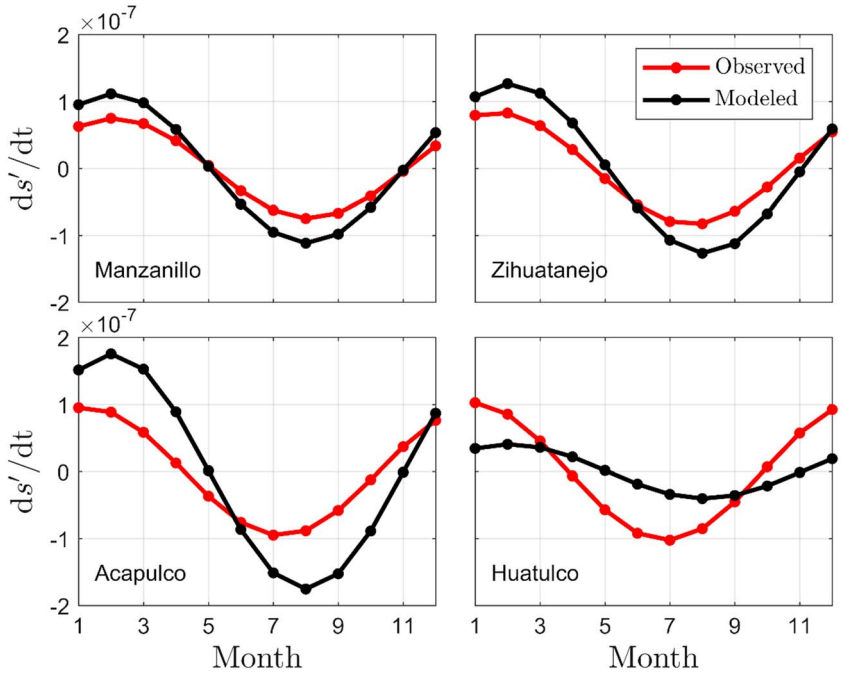

Figure 8. Annual observed and modeled salinity tendency (g kg^{-1} s^{-1}) in the four domains.

approximates it to the observations. In the other domains, the inclusion of the entrainment in the model either had no significant effect or it did not improve the model accuracy.

5. Discussion

5.1. Steady Balance

In the mean, Huatulco, Zihuatanejo, and Manzanillo are domains of net evaporation. In Acapulco, the local net precipitation seems an isolated feature, but it corresponds with the northern edge of a coastal strip of net precipitation (not shown) that originates at the Gulf of Panama. This feature is usually not resolved by the large-scale studies in the ETP like those of Fiedler and Talley (2006) and Amador et al. (2006). The spatial continuity of this alongshore feature is only interrupted in the vicinity of the gulfs of Tehuantepec and Papagayo, where the influence of the semipermanent strong winds produces a local strong net evaporation (Amador et al., 2006) and a related locally increase of salinity (Figure 2). This local feature produces an equatorward salinity increase in Huatulco that is exacerbated by the choice of the domain limits (i.e., this effect would not have been noticed the limit between Acapulco and Huatulco. for example, southern). In contrast, in the AM region the salinity increases poleward across a strong front caused by the confluence of the fresh surface waters from the tropical area with the saltier waters that outflow from the Gulf of California (Portela et al., 2016).

The mean modeled alongshore component of the velocity ($\overline{v}_m$; Figure 5c) obtained from the salinity balance coincides with the previous findings on the regional circulation. The mean poleward circulation in Manzanillo and Zihuatanejo agrees with the northward coastally trapped flow result of Sverdrup dynamics between 17°N and 20°N (Godínez et al., 2010). The equatorward $\overline{v}_m$ in Huatulco is consistent with the flow on the northeastern edge of the Tehuantepec Bowl between approximately 96–98°W and 15–16°N (Kessler, 2006). The weak $\overline{v}_m$ in Acapulco therefore represents the transition between these two distinct alongshore circulation regimes and suggests that the mean flow perpendicular to the coast could be important in this domain.

These results suggest that the mean MCC is decoupled from the Tehuantepec region and that the salinity budget in this region is largely described by the balance between the $E - P$ and the

Table 2
Amplitudes and Phases of the Annual Fit of the Observed and Modeled Salinity Tendency

	Amplitude (× 10^{-7})		Phase (month)	
	Observed	Modeled	Observed	Modeled
Manzanillo	0.75±0.2	1.12±0.3	1.6±0.6	1.5±1.0
Zihuatanejo	0.84±0.2	1.27±0.3	1.1±0.5	1.6±1.2
Acapulco	0.96±0.3	1.76±0.5	0.7±0.5	1.5±1.0
Huatulco	1.03±0.3	0.40±0.3	0.4±0.5	1.6±1.2

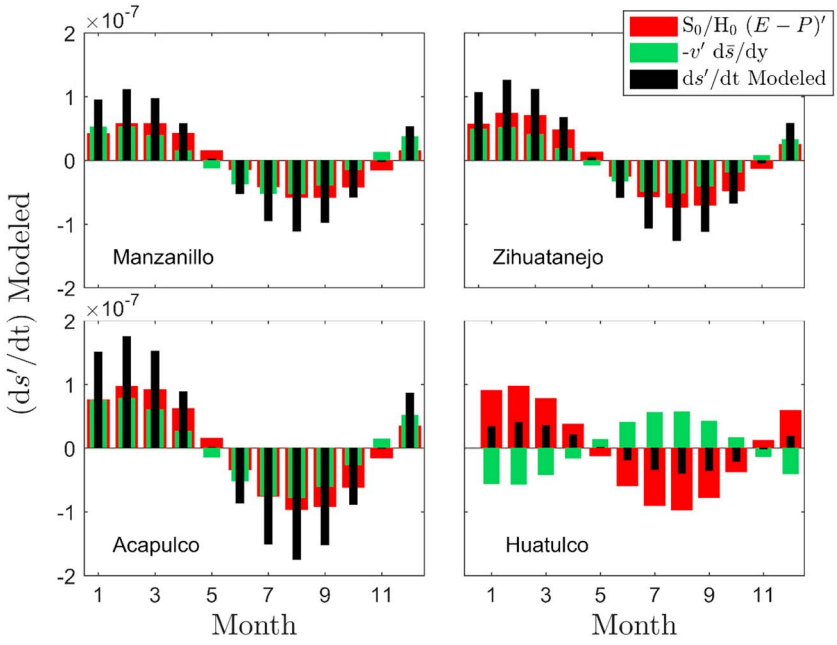

Figure 9. Annual salinity tendency (s^{-1}) in each domain (black bars), as the sum of the linearized, one-dimensional advection term (green bars) and the freshwater flux (red bars).

alongshore salt advection. In a region such as the TPOM with a complicated circulation regime, it is of great utility to know that with these only two terms, which can be easily calculated, the salinity balance can be well approximated.

5.2. Temporal Variability

The model results suggest that the salt advection between the GoT and Cabo Corrientes is driven by the time-dependent variability of the alongshore velocity and a mean salinity (Figure 6, term IV). Since the annual and seasonal signals of the alongshore velocity between the GoT and Cabo Corrientes are well represented by the MCC (Godínez et al., 2010; Portela et al., 2016), this current was pointed out as the principal agent responsible for the salt advection between those points, as suggested by Portela et al. (2016) In contrast, the low salt advection perpendicular to the coast agrees with the predominance of the alongshore currents in this region. Beron-Vera and Ripa (2002) also suggested the importance of this term when they found the advection from the Pacific Ocean to be the predominant factor determining the salinity balance inside the Gulf of California.

Both the modeled and the observed annual salinity tendency show strong spatial continuity in the AM region that suggests that these three northern domains are driven by similar dynamics. The sum of the mean plus the annual advection produce, mainly in Manzanillo, a net poleward salt advection during most of the year (Figures 5 and 8), which means that tropical waters are being advected poleward by the annual MCC mainly during summer. This result is consistent with the summer/fall surface salinity minimum and the saltier winter/spring characteristics of the water masses observed in the TPOM by Portela et al. (2016).

Table 3
Relative Contribution of the Freshwater Flux, Linear, One-Dimensional Advection, and Entrainment Terms to the Seasonal Salinity Tendency Model in Each Domain

	Explained variance			
	Manzanillo	Zihuatanejo	Acapulco	Huatulco
$\frac{S_o}{H_o}(E-P)'$	49%	58%	48%	67%
$-v'\frac{\partial \bar{S}}{\partial y'}$	49%	37%	39%	28%
Entrainment	2%	5%	13%	4%

While the freshwater flux and the annual alongshore velocity (i.e., the MCC) are in phase across all four domains (Figure 4), the modeled salt advection in Huatulco is decoupled from the AM region (Figure 9). Rather than a real feature, the change in the sense of the salt advection in this domain is related to the local equatorward increase of the mean salinity (Figure 2b) exacerbated by the choice of the domain limits. The result is a poor model representation of the annual observed salinity tendency near the GoT (Figure 8).

Since the climatologies of all the variables considered in the salinity balance show strong seasonal signals, this time scale is considered to

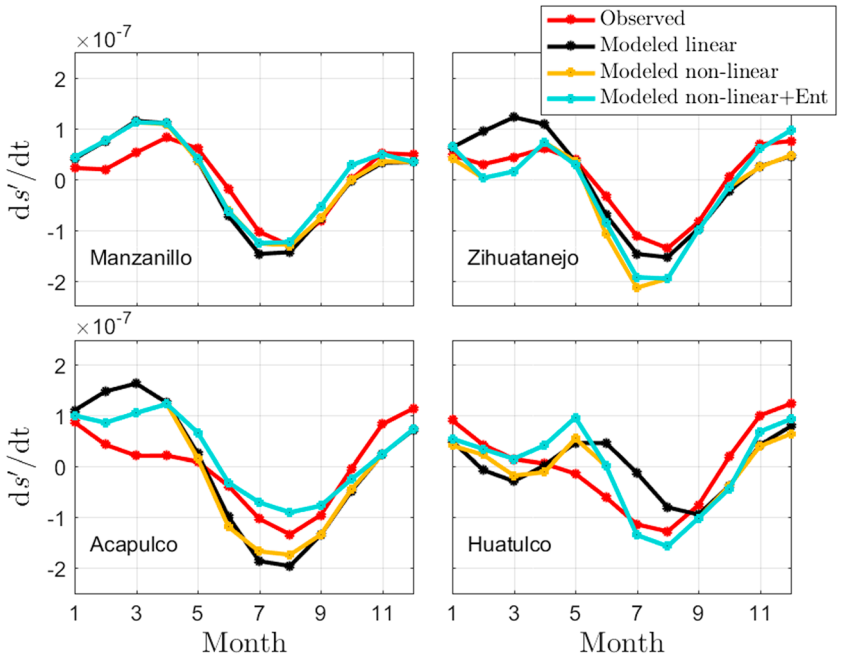

Figure 10. Seasonal observed and modeled salinity tendency (g kg^{-1} s^{-1}) in the four model domains with and without the inclusion of the nonlinear and entrainment terms.

dominate the total variability. Based on this assumption, the relative contributions of all terms to the salinity tendency may be quantified. The analysis showed that both the salt advection and the freshwater flux must be taken into account when studying the spatial and/or temporal salinity variations in this area while entrainment has less importance and mixing is negligible. Although the minor role of the entrainment was expected given the small monthly variations of the MLD in the study area, the neglection of the velocity perpendicular to the coast is a rough approximation. It could be responsible for the lack of improvement of the model accuracy when the entrainment was introduced in the computations.

In general terms the seasonal salinity model is dominated by the annual signal. However, the semiannual harmonic greatly improves its accuracy in representing the observations between May and January, and it has effect mainly on the model's phase. Annual and semiannual harmonics are in phase during summer in Manzanillo and Zihuatanejo, reinforcing the loss of salinity between June and September. Gómez-Valdivia et al. (2015) found, using a numerical model, an important subsurface semiannual signal of the MCC related with the passage of semiannual Kelvin waves. However, this is the first time that the effect of this signal is reported within the mixed layer and further investigation is needed to identify the forcings responsible for this signal.

Between February and April, the model does not reproduce well the observed salinity tendency. The variability explained by Term III of equation (7) was nearly zero in Acapulco, and its neglect has no effect on the results. However, the omission of the advection perpendicular to the coast is more likely to be responsible for this imbalance. Unlike in summer and fall, when the alongshore MCC is strong and dominates the circulation in the region, in winter and spring the MCC weakens and the circulation loses the alongshore predominance. Acapulco also coincides with the northern edge of the Tehuantepec Bowl that has an appreciable component perpendicular to the coast. This is also reflected in the low mean value of the alongshore velocity in this domain (Figure 2).

In Huatulco, while the annual model did not reproduce the observations well, the semiannual signal plays a significant role in the salinity balance. Its inclusion in the model greatly improves the estimates in fall and winter. In addition, the nonlinear processes are revealed as key in this domain in summer to adjusting the phase of the model to the observations. The Ekman transport might be involved in the nonlinear salt advection since it is directly related to the wind stress that is strong in this area. In addition, strong Ekman pumping

velocity and upwelling events have also been reported in the vicinity of the GoT. In Acapulco and Huatulco, where there is a strong vertical salinity gradient (fresh waters overlay saltier subsurface waters) between 30 and 75 m the whole year (Portela et al., 2016), upwelling could be important (Chapa-Balcorta et al., 2015; Kessler, 2006). This process could potentially smooth the salinity tendency, which is in agreement with the effect that the entrainment term has in Acapulco (Figure 10, blue line).

Relatively intense upwelling has been also reported around Cabo Corrientes, near the domain of Manzanillo, mostly in the first half of the year (Kurczyn et al., 2012). However, the differences between the salinity at surface and in deeper layers of the water column in this locality are small compared to those in summer and fall (Portela et al., 2016) when, in turn, there is no significant upwelling. This is in agreement with the lack of importance of the entrainment and nonlinear terms in Manzanillo, where salinity tendency is largely reproduced by the annual linear model.

Although it has been pointed out that the fact of considering only the alongshore advection is probably the main cause of the model imbalance, it is important to remind that other factors related to the data processing, such as averaging, interpolation, and errors associated to the computations and to the harmonic fit, are an important source of uncertainty. Figures S1 and S2 (supporting information) show the uncertainty of the estimations of the seasonal signal for both the observed and modeled salinity tendency. In general terms, the seasonal fit is good, as expected due to the high percentage of variance explained by the seasonal signal of the climatological variables (Table 1).

Other factors as the temporal averaging involved in the elaboration of the monthly climatology seem to be a more important source of imbalance. This averaging masks, for example, the interannual time scale and the mesoscale features. The latter has been reported to be dominant in the vicinity of the GoT (Barton et al., 2009; Chapa-Balcorta et al., 2015; Trasviña & Barton, 2008; Trasviña et al., 1995). Godínez et al. (2010) suggested that from Cabo Corrientes toward the southeast, mesoscale variability increases while seasonal variability decreases and preliminary results of this study confirm this behavior. We calculated the variance explained by the seasonal signal of the geostrophic velocity from the complete time series (~ 20 years of data every ~10 days). This variance increases from 24% in Huatulco to 38% in Manzanillo. As expected, the difference between these values and those of the variance explained by the seasonal signal of the climatological velocity (~ 90% in all the domains, Table 1) is important and it gives an idea of the amount of variability that is not accounted for by the climatology.

The results presented here about the relative importance of the freshwater fluxes and the main dynamical processes at climatological time scales in the TPOM are important to understand the life strategy of the marine organisms regarding spawning periods, habitat occupation, or migration routes among others.

Future studies could evaluate the effect that the salinity tendency has on the marine life at longer time scales from the results presented here. However, they also provide a new insight on previous works. León-Chávez et al. (2010) found, during November of 2005, in the TPOM, a larval fish assemblage associated to waters with unexplained warm and fresh characteristics. With the present results, we can explain that during November, tropical surface water is advected northward by the MCC defining a new habitat with tropical characteristics.

5.3. Overview

The previous studies on the salinity balance and distribution including the ETP covered large spatial and temporal scales using coarse grids and, therefore, do not resolve well the coastal areas. In coastal regions, where satellite data are less reliable, the relative general scarcity of salinity data had typically limited the resolution and the accuracy of the salinity balance computations. Regional studies based on observations can be only carried out in well-sampled areas as it is the case of the Gulf of California (Beron-Vera & Ripa, 2002). This is the first time that enough hydrographic data have been collected in the TPOM to solve the mean and time-dependent mixed-layer salinity balance.

The present results show how in a region with complicated dynamics the salt advection can be well approximated by only the seasonal alongshore current represented by the MCC. The importance of this result resides in the convenience of identifying and isolating the two main processes more relevant for the salinity balance without the necessity of complicated computations or data collection. Salinity is an important variable in different branches of the ocean sciences involving physical and geochemical properties and plankton

distribution. Therefore, ongoing and future research in the TPOM, a region of burgeoning oceanographic interest, will benefit from the results presented here.

6. Concluding Remarks

A simplified analytical model of the TPOM was able to identify and describe for the first time the main processes involved in the mixed-layer salinity balance between the GoT and Cabo Corrientes.

The mixed-layer salinity tendency in the steady state is well approximated by the balance between only the freshwater flux and the salt advection.

The seasonal model reproduces well the observations between May and January in all four domains, while the winter season is poorly resolved. The nonlinear advection is most important in winter, when it approximates the model amplitude to the observations, and in the Huatulco domain.

The region between Acapulco and Manzanillo is driven by the same dynamics, with the MCC as the main forcing responsible for the seasonal salt advection. This region loses salinity between June and October as the result of net precipitation and poleward advection of fresh tropical waters. Although the freshwater flux varies, the MCC is also present in Huatulco, so its area of generation is placed southeast of this domain, but it cannot be stablished in this study.

The salinity balance in all four domains is achieved by similar contributions of the alongshore salt advection and freshwater flux, while the entrainment had only a sporadic and local effect.

Acknowledgments
The hydrographic data supporting this work are available in the WOD13 database (https://www.nodc.noaa.gov/OC5/WOD13/). Data of most of the cruises are available in http://usuario.cicese.mx/~mxcali/curriculum/curriculum.html as well as upon request to Emilio Beier (ebeier@cicese.mx). The satellite data can be downloaded at CTOH/LEGOS website (http://ctoh.legos.obs-mip.fr/products/coastal-products), and the $E - P$ data are available in https://rda.ucar.edu/datasets/ds093.0/. This is a product of the project *Un estudio de la Corriente Costera Mexicana y el Pacífico adyacente, con un SeaGlider, cruceros oceanográficos y datos de satélite* supported by CONACyT (SEP2011–168034-T). Funding to this work was also provided by CONACyT through the grant 329234 awarded to Esther Portela. We also thank NOAA/National Marine Fisheries Service/Southwest Fisheries Science Center that provided the CTD and thermosalinograph data as described by Philbrick et al. (2001) and Jackson et al. (2004).

References

Amador, J. A., Alfaro, E. J., Lizano, O. G., & Magaña, V. O. (2006). Atmospheric forcing of the eastern tropical Pacific: A review. *Progress in Oceanography*, *69*(2–4), 101–142. https://doi.org/10.1016/j.pocean.2006.03.007

Barton, E. D., Lavín, M. F., & Trasviña, A. (2009). Coastal circulation and hydrography in the Gulf of Tehuantepec, Mexico, during winter. *Continental Shelf Research*, *29*(2), 485–500. https://doi.org/10.1016/j.csr.2008.12.003

Beron-Vera, F. J., Olascoaga, M. J., & Goni, G. J. (2008). Oceanic mesoscale eddies as revealed by Lagrangian coherent structures. *Geophysical Research Letters*, *35*, L12603. https://doi.org/10.1029/2008GL033957

Beron-Vera, F. J., & Ripa, P. (2002). Seasonal salinity balance in the Gulf of California. *Journal of Geophysical Research*, *107*(C8), 1–15. https://doi.org/10.1029/2000JC000769

Chapa-Balcorta, C., Hernandez-Ayon, J. M., Durazo, R., Beier, E., Alin, S. R., & López-Pérez, A. (2015). Influence of post-Tehuano oceanographic processes in the dynamics of the CO_2 system in the Gulf of Tehuantepec, Mexico. *Journal of Geophysical Research: Oceans*, *120*, 7752–7770. https://doi.org/10.1002/2015JC011249

Cronin, M. F., & McPhaden, M. J. (1998). Upper ocean salinity balance in the western equatorial Pacific. *Journal of Geophysical Research*, *103*(C12), 27,567–27,587. https://doi.org/10.1029/98JC02605

Da-Allada, C. Y., Alory, G., Penhoat, Y., Kestenare, E., Durand, F., & Hounkonnou, N. M. (2013). Seasonal mixed-layer salinity balance in the tropical Atlantic Ocean: Mean state and seasonal cycle. *Journal of Geophysical Research: Oceans*, *118*, 332–345. https://doi.org/10.1029/2012JC008357

Delcroix, T., Henin, C., Porte, V., & Arkin, P. (1996). Precipitation and sea-surface salinity in the tropical Pacific Ocean. *Deep Sea Research, Part I*, *43*(7), 1123–1141. https://doi.org/10.1016/0967-0637(96)00048-9

Dessier, A., & Donguy, J. R. (1994). The sea surface salinity in the tropical Atlantic between 10°S and 30°N—Seasonal and interannual variations (1977–1989). *Deep Sea Research Part I: Oceanographic Research Papers*, *41*(1), 81–100. https://doi.org/10.1016/0967-0637(94)90027-2

Dong, S., Garzoli, S. L., & Baringer, M. (2009). An assessment of the seasonal mixed layer salinity budget in the Southern Ocean. *Journal of Geophysical Research*, *114*, C12001. https://doi.org/10.1029/2008JC005258

Fiedler, P. C., & Talley, L. D. (2006). Hydrography of the eastern tropical Pacific: A review. *Progress in Oceanography*, *69*(2–4), 143–180. https://doi.org/10.1016/j.pocean.2006.03.008

Foltz, G. R., & McPhaden, M. J. (2008). Seasonal mixed layer salinity balance of the tropical north Atlantic Ocean. *Journal of Geophysical Research*, *113*, C02013. https://doi.org/10.1029/2007JC004178

Franco, A. C., Hernández-Ayón, J. M., Beier, E., Garçon, V., Maske, H., Paulmier, A., et al. (2014). Air-sea CO_2 fluxes above the stratified oxygen minimum zone in the coastal region off Mexico. *Journal of Geophysical Research: Oceans*, *119*, 1–15. https://doi.org/10.1002/2013JC009337.Received

Godínez, V. M., Beier, E., Lavín, M. F., & Kurczyn, J. A. (2010). Circulation at the entrance of the Gulf of California from satellite altimeter and hydrographic observations. *Journal of Geophysical Research*, *115*, C04007. https://doi.org/10.1029/2009JC005705

Gómez-Valdivia, F., Parés-Sierra, A., & Flores-Morales, A. L. (2015). The Mexican Coastal Current: A subsurface seasonal bridge that connects the tropical and subtropical northeastern Pacific. *Continental Shelf Research*, *110*, 100–107. https://doi.org/10.1016/j.csr.2015.10.010

Jackson, A., Gerrodette, T., Chivers, S., Lynn, M., Olson, P., & Rankin, S. (2004). Marine mammal data collected during a survey in the eastern tropical Pacific Ocean aboard the NOAA ships McArthur LI and David Starr Jordan, July 29–December 10, 2003.

Johnson, E. S., Lagerloef, G. S. E., Gunn, J. T., & Bonjean, F. (2002). Surface salinity advection in the tropical oceans compared with atmospheric freshwater forcing: A trial balance. *Journal of Coastal Research*, *107*(C12), SRF 15-1–SRF 15-11. https://doi.org/10.1029/2001JC001122

Kara, A. B., Rochford, P. A., & Hurlburt, H. E. (2000). An optimal definition for ocean mixed layer depth. *Journal of Geophysical Research*, *105*(C7), 16,803–16,821. https://doi.org/10.1029/2000JC900072

Kessler, W. S. (2006). The circulation of the eastern tropical Pacific: A review. *Progress in Oceanography*, *69*(2–4), 181–217. https://doi.org/10.1016/j.pocean.2006.03.009

Kjerfve, B., Schettini, C. A. F., Knoppers, B., Lessa, G., & Ferreira, H. O. (1996). Hydrology and salt balance in a large, hypersaline coastal lagoon: Lagoa de Araruama, Brazil. *Estuarine, Coastal and Shelf Science*, *42*(6), 701–725. https://doi.org/10.1006/ecss.1996.0045

Kurczyn, J. A., Beier, E., Lavín, M. F., & Chaigneau, A. (2012). Mesoscale eddies in the northeastern Pacific tropical-subtropical transition zone: Statistical characterization from satellite altimetry. *Journal of Geophysical Research*, *117*, C10021. https://doi.org/10.1029/2012JC007970

Lavín, M. F., Beier, E., Gómez-Valdés, J., Godínez, V. M., & García, J. (2006). On the summer poleward coastal current off SW México. *Geophysical Research Letters*, *33*, L02601. https://doi.org/10.1029/2005GL024686

León-Chávez, C. A., Sánchez Velasco, L., Beier, E., Lavín, M. F., Godínez, V. M., & Farber Lorda, J. (2010). Larval fish assemblages and circulation in the Eastern Tropical Pacific in Autumn and Winter. *Journal of Plankton Research*, *32*(4), 397–410. https://doi.org/10.1093/plankt/fbp138

McDougall, T. J., & Barker, P. M. (2011). Getting started with TEOS-10 and the Gibbs Seawater (GSW) Oceanographic Toolbox. SCOR/IAPSO WG127 (28 pp.). Retrieved from http://www.teos-10.org/pubs/Getting_Started.pdf

Montes, J. M., Lavin, M. F., & Parés-Sierra, A. (2015). Seasonal heat and salt balance in the upper Gulf of California. *Journal of Coastal Research*, *320*, 853–862. https://doi.org/10.2112/JCOASTRES-D-14-00192.1

Pantoja, D., Marinone, S. G., Parés-Sierra, A., & Valdivia, F. G. (2012). Numerical modeling of seasonal and mesoscale hydrography and circulation in the Mexican central Pacific. *Ciencias Marinas*, *38*(2), 363–379. https://doi.org/10.7773/cm.v38i2.2007

Philbrick, V. A., Fiedler, P. C., Fluty, J. T., & Reilly, S. B. (2001). Report of oceanographic studies conducted during the 2000 eastern tropical Pacific Ocean survey on the research vessels David Starr Jordan and McArthur.

Portela, E., Beier, E., Barton, E. D., Castro, R., Godínez, V., Palacios-Hernández, E., et al. (2016). Water masses and circulation in the tropical Pacific off central Mexico and surrounding areas. *Journal of Physical Oceanography*, *46*(10), 3069–3081. https://doi.org/10.1175/JPO-D-16-0068.1

Ren, L., & Riser, S. C. (2009). Seasonal salt budget in the northeast Pacific Ocean. *Journal of Geophysical Research*, *114*, C12004. https://doi.org/10.1029/2009JC005307

Romero-Centeno, R., Zavala-Hidalgo, J., Gallegos, A., & O'Brien, J. J. (2003). Isthmus of Tehuantepec wind climatology and ENSO signal. *Journal of Climate*, *16*(15), 2628–2639. https://doi.org/10.1175/1520-0442(2003)016<2628:IOTWCA>2.0.CO;2

Saraceno, M., Strub, P. T., & Kosro, P. M. (2008). Estimates of sea surface height and near-surface alongshore coastal currents from combinations of altimeters and tide gauges. *Journal of Geophysical Research*, *113* L11605 1–20. https://doi.org/10.1029/2008JC004756

Trasviña, A., & Barton, E. D. (2008). Summer circulation in the Mexican tropical Pacific. *Deep-Sea Research Part I: Oceanographic Research Papers*, *55*(5), 587–607. https://doi.org/10.1016/j.dsr.2008.02.002

Trasviña, A., Barton, E. D., Brown, J., Velez, H. S., Kosro, P. M., & Smith, R. L. (1995). Offshore wind forcing in the Gulf of Tehuantepec, Mexico: The asymmetric circulation. *Journal of Geophysical Research*, *100*(C10), 649–663.

Wen, C., Xue, Y., & Kumar, A. (2012). Ocean-atmosphere characteristics of tropical instability waves simulated in the NCEP climate forecast system reanalysis. *Journal of Climate*, *25*(18), 6409–6425. https://doi.org/10.1175/JCLI-D-11-00477.1

Wyrtki, K. (1965). Surface currents of the eastern tropical Pacific Ocean. *Inter-American Tropical Tuna Comission*, *9*(5), 271–304.

Yu, L. (2011). A global relationship between the ocean water cycle and near-surface salinity. *Journal of Geophysical Research*, *116*, C10025. https://doi.org/10.1029/2010JC006937

Yu, L., Jin, X., Josey, S. A., Lee, T., Kumar, A., Wen, C., & Xue, Y. (2017). The global ocean water cycle in atmospheric reanalysis, satellite, and ocean salinity. *Journal of Climate*, *30*(10), 3829–3852. https://doi.org/10.1175/JCLI-D-16-0479.1

Yu, Z., McCreary, J. P., Yaremchuk, M., & Furue, R. (2008). Subsurface salinity balance in the South China Sea. *Journal of Physical Oceanography*, *38*(2), 527–539. https://doi.org/10.1175/2007JPO3661.1